Dynamics of transcription induced by osmostress promoters revealed by live single-cell assays

Victoria Wosika and Serge Pelet*

Department of Fundamental Microbiology, University of Lausanne, 1015 Lausanne, Switzerland.

*Correspondance : serge.pelet@unil.ch

Abstract

Precise regulation of gene expression in response to environmental changes is crucial for cell survival, adaptation and proliferation. In eukaryotic cells, extracellular signal integration is often carried out by Mitogen-Activated Protein Kinases (MAPK), which control cell differentiation, apoptosis and stress response. Despite a robust MAPK signaling activity, downstream gene expression can display a great variability between single cells. We have used *Saccharomyces cerevisiae* to study the dynamics of transcription of stress-responsive genes. Following a hyper-osmotic shock, the MAPK Hog1 induces the transcription of hundreds of genes. Using a PP7 reporter assay, we have monitored with high temporal resolution and in single cells, the dynamics of transcription from a set of promoters in order to highlight how the onset, the level and the shutoff of transcription are regulated in this model MAPK pathway.

Keywords

MAPK signaling, HOG pathway, Transcription, Single-cell analysis, fluorescence microscopy, PP7 phage coat protein.

Introduction

A crucial function to all cellular life is the ability to sense the environment and adapt to its variations. These changes in the extracellular environment will induce specific cellular responses. These responses are orchestrated by signal transduction cascades which receive cues from plasma membrane sensors and turn this information into a biological response by inducing complex transcriptional programs implicating hundreds of genes[1–3]. Tight regulation of signaling is crucial to ensure the correct temporal modulation of gene transcription, which can otherwise alter the cell physiology[4–6]. Interestingly, single-cell analyses have revealed that genes regulated by an identical signaling activity can display a wide variability in their transcriptional responses[7–10]. This noise in transcriptional output questions how signal transduction can faithfully induce different loci and which molecular mechanisms contribute to this variability in gene expression.

In eukaryotic cells, various environmental stimuli are transduced by the highly conserved Mitogen-Activated Protein Kinases (MAPK) cascades[11,12]. In *Saccharomyces cerevisiae*, a sudden increase in the osmolarity of the medium is

sensed by the High Osmolarity Glycerol (HOG) pathway, which leads to the activation of the MAPK Hog1, a homolog of p38 in mammals[13,14]. Upon hyper-osmotic stress, the kinase activity of Hog1 drives an increase in the internal glycerol concentration allowing balancing of the internal and the external osmotic pressures, promoting the adaptation of the cells to their new environment. In parallel to its cytoplasmic activity, Hog1 also transiently accumulates into the cell nucleus to induce the expression of hundreds of osmostress-responsive genes (Figure 1A). The MAPK is recruited to promoter regions by Transcription Factors (TF) and, in turn, Hog1 recruits chromatin remodeling and modifying complexes, the Pre-Initiation Complex and the RNA Polymerase II (PolII) to trigger gene expression[15,16]. Once cells have adapted, Hog1 is inactivated and exits the cell nucleus, transcription stops and chromatin is rapidly reassembled at HOG-induced gene loci.

Biochemical analyses of this pathway have identified the key players implicated in the induction of gene expression and the central role played by the MAPK in all these steps[15]. In parallel, single-cell measurements have uncovered the large variability present in the expression of stress-responsive genes. In particular, translational reporters and RNA-FISH measurements have helped identify that slow chromatin remodeling at each locus is generating strong intrinsic noise in the gene expression of many stress-responsive genes[9,17]. In order to get deeper insights into the chromatin regulation of osmostress gene expression kinetics, we aimed at monitoring the dynamics of mRNA production of osmostress-responsive genes in live single cells. Since a decade, phage coat protein-based assays, like the MS2 or PP7 systems, have been used to visualize mRNA production in live single cells[18,19]. These experiments contributed to reveal the bursty nature of transcription, whereby a set of polymerases simultaneously transcribing a gene generates a burst in mRNA production, which is followed by a pause in transcription[20–22].

In this study, we dissect the kinetics of transcription of osmostress genes. The production of mRNA was monitored using a fluorescent phage coat protein assay. This reporter allowed us to monitor with high temporal resolution and in a fully automated manner, the fluctuations in transcription arising in hundreds of live single cells. The analysis of the characteristic responses of multiple stress-responsive promoters allowed us to identify some general rules that govern the initiation, the level and the shutoff of the transcriptional process.

Results

High osmotic pressure is sensed and transduced in the budding yeast *Saccharomyces cerevisiae* via the HOG signaling cascade, which culminates in the activation of the MAPK Hog1 (Figure 1A). Upon activation, this key regulator accumulates in the nucleus to trigger gene expression in a stress level-dependent manner (Supplementary Fig 1A). The activity of the kinase can thus be monitored by following its own nuclear enrichment[23,24]. In parallel to Hog1, the general stress response pathway is induced by the hyper-osmotic shock and its main transcription factors Msn2/4 also relocate into the nucleus with dynamics highly similar to the ones observed for Hog1 (Supplementary Fig 1B and C)[25,26]. Nuclear Hog1 and Msn2/4 serve as triggers for osmostress genes expression with approximately 250 genes being up-

regulated by this stimulus[1,27]. The activity of the pathway, and thus gene expression, is limited to the cellular adaptation time which can be followed by monitoring Hog1 nuclear exit or the recovery of the cell size (Supplementary Fig 1A and D). The fast and transient activity of the osmostress response as well as the homogenous activation of the MAPK within the population[9,24] make this signaling pathway an excellent model for understanding the induction of eukaryotic stress-responsive genes, which are often accompanied by important chromatin remodeling.

Monitoring osmostress gene transcription dynamics

In order to quantify the production of mRNA in live single cells, we used the PP7 system to label mRNAs[19]. Briefly, constitutively expressed and fluorescently labeled PP7 phage coat proteins associate to a binding partner: an mRNA-encoded array of twenty-four PP7 stem loops (PP7sl). In our settings, this reporter construct is integrated in the genome at the *GLT1* locus, downstream of a promoter of interest (Figure 1B)[19], in a strain bearing a nuclear tag (Hta2-mCherry) and expressing a fluorescently tagged PP7 allele (PP7ΔFG-GFPenvy[28,29] (PP7-GFP), Methods). Upon activation of the promoter, local accumulation of newly synthesized transcripts at the Transcription Site (TS) leads to the formation of a bright fluorescent focus due to the enrichment in PP7-GFP fluorescence above the background signal (Figure 1C and Supplementary Movie 1). The fluorescence intensity at the TS is proportional to the number of mRNA being transcribed at this locus and thus to the instantaneous load of RNA polymerases. After termination, single mRNAs are exported out the nucleus and their fast diffusion in the cytoplasm prevents their detection under the selected illumination conditions (Methods).

Typically, time-lapse imaging with fifteen-second intervals for twenty-five minutes with six Z-planes for the PP7-GFP channel on four fields of view was performed (Methods). All microscopy acquisitions were performed as independent duplicate or triplicate experiments. Image segmentation and quantification were performed automatically, allowing to extract typically one hundred to three hundred single-cell traces for each experiment[30]. The mean intensity of the 20 brightest pixels in the nucleus from which the average cell fluorescence was subtracted, was used as a measurement of TS fluorescence and thus as proxy for transcriptional activity (Figure 1D and E, Methods).

Figure 1D displays the average TS fluorescence from at least 190 cells bearing the p*STL1*-PP7sl reporter following activation of the HOG pathway by various NaCl concentrations. The *STL1* promoter is one of the most studied HOG-induced promoters and displays strong intrinsic noise[9,31–33]. As expected, increasing salt concentration leads to an increasing transcriptional output from the cell population and no change in TS fluorescence is detected in the medium control. The dynamics observed are in agreement with control experiments performed with a dynamic protein expression reporter (dPSTR, Supplementary Fig 2A) and with previously published results[33,34]. Importantly, in a reporter strain where we combined the p*STL1*-PP7sl reporter and the Hog1-mCherry relocation assay, we observe an absence of correlation between the two assays (Supplementary Fig 3). Cells with similar Hog1 relocation behaviors can display highly variable transcriptional outputs. Because we cannot infer the downstream PP7 response from the Hog1 activity pattern, we

concentrated our analysis on strains bearing only the PP7 reporter system, allowing to sample the TS dynamics with higher frequency and in more cells.

The hundreds of dynamic single-cell measurements acquired with the PP7sl reporter form a very rich dataset where multiple features can be extracted from each trace (Figure 1E, Methods). Our analysis allows to reliably quantify the appearance and disappearance (Start Time and End Time) of the TS (Supplementary Fig 4). The maximum intensity of the trace and the integral under the curve provide estimates of the transcriptional output from each promoter. In addition, we have identified transcriptional bursts when monitoring strong fluctuations in the TS intensity.

HOG genes are expressed with a variety of transcription dynamics

In addition to p*STL1*, five other stress-responsive promoters, often used in the literature to report on HOG pathway transcriptional activity, were selected for this study[32,35]. Each strain differs only by the one thousand base pairs of the promoters present in front of the PP7sl (800bp for p*STL1*[9,36]); however, each strain displays a different transcriptional response following a 0.2M NaCl stimulus (Figure 2A). Because the level of accumulation of the PP7 signal at the transcription site and the timing of the appearance and disappearance of the TS is different for each tested promoter, it implies that the promoter sequence dictates multiple properties of the transcription dynamics. These dynamics are in line with control experiments performed with the dPSTR assay (Supplementary Fig 2B) and population-averaged responses published in the literature[32,34].

Because the PP7 assay relies on the binding of free phage coat proteins, we generated strains expressing three times more phage-coat proteins and quantified the transcriptional response for the two promoters with the highest expression levels (p*GPD1* and p*HSP12*, Supplementary Fig 5). The single-cell parameters recovered between the overexpressed and our standard reporters are highly similar, denoting the absence of titration of the assay under our experimental conditions.

The automated analysis allows to identify the presence or absence of a transcription site in each single cell, and thus the fraction of cells that induce the promoter of interest (Figure 2B). Interestingly, even in absence of stimulus, some promoters display a basal level of transcription. In the p*GRE2*, p*HSP12* and p*GPD1* reporter strains, in 5 to 20% of the cells, an active transcription site can be detected in the few time points before the stimulus (Figure 2C, upper image and Supplementary Movie 2). If the period of observation is extended to a twenty-five-minute time lapse without stimulus, this fraction increases 2 to 3-fold (Supplementary Fig 6). Upon activation by 0.2M NaCl, the fraction of responding cells for the three promoters that display basal expression surpasses 85%, while for the three promoters without basal induction (p*ALD3*, p*CTT1* and p*STL1*), the fraction of responding cells remains below 65%. The partial activation of the HOG-responsive promoters in the cell population is in agreement with previous studies which observed a bimodal expression pattern in the hyper-osmotic stress response pathway[9,17].

A key parameter controlled by the promoter sequence is the timing of induction. In Figure 2D, the time when cells become transcriptionally active (Start Time) is plotted as a Cumulative Distribution Function (CDF) only for the cells where a TS is detected

after the stimulus, thereby excluding basal expressing cells and non-responding cells. Treatment with 0.2M NaCl results in a sudden activation of transcription (Figure 2D). This contrasts with non-induced samples, where the CDF of the promoters displaying basal activity rises almost linearly, because cells stochastically activate transcription during the measurement window (Supplementary Fig 6C). Upon stress, the promoters displaying basal activity tend to be induced faster than the promoters that are repressed under log-phase growth, with p*GPD1* being activated the fastest (~1 min), while p*ALD3* and p*STL1* require more than 4 minutes for activation (Figure 2E). However, there is a great variability in transcription initiation between cells of the same population, since we observe 3 to 4 minutes delay between the 10th and 90th percentiles of the population, with the exception of p*GPD1* where the induction is more uniform, and less than 2 min delay is observed (Figure 2E). Comparison between individual replicates demonstrates the reliability of our measurement strategy. The 10th and 50th percentiles of Start Time for the promoters with a basal expression are significantly faster than at least two or all three of the promoters lacking basal expression.

Interestingly, we observe a correlation between faster transcriptional activation from p*GPD1*, p*HSP12* and p*GRE2* and the presence of basal expression level. Moreover, these promoters also display the higher number of responding cells upon a 0.2M NaCl shock. These results suggest that basal expression is associated with a more permissive chromatin state. Thus, promoters with basal activity display a lower transcriptional activation threshold, which leads to a faster activation and higher probability of being induced.

To test this hypothesis, we disrupted the function of the chromatin remodeling complex SAGA by deleting *GCN5*[37], which led to fewer transcribing cells and slower induction of the p*STL1* reporter (Figure 2F). However, abolishing histone H2AZ variants exchange mainly at +1 and -1 nucleosomes by deleting *HTZ1* [38,39] results only in a reduction in the fraction of transcribing cells. Conversely, the chromatin state at the *STL1* promoter can be loosened by relieving the glucose repression when using raffinose as a C-source[40]. A fraction of the cells grown in these conditions displays basal expression from the p*STL1* reporter. Upon stimulation with 0.2M NaCl, the median Start Time is accelerated by 1 min in raffinose compared to glucose (Figure 2G).

Together these results reinforce the idea that there is a close link between the chromatin state under log-phase growth and the ability to induce stress-responsive genes. A promoter that is tightly repressed will need more Hog1 activity and thus more time to become transcriptionally active, therefore displays a lower fraction of responding cells.

Early Hog1 activity dictates transcriptional competence

Surprisingly, the large majority of the measured Start Times fall within the first few minutes of Hog1 activity. The total period of Hog1 activity provides a temporal window where transcription can potentially be initiated. However, the switch to a transcriptionally active state takes place almost exclusively within the first few minutes after the stimulus. Figure 3A compares the characteristic timing of the Hog1 nuclear

enrichment behavior at three different NaCl concentrations (Supplementary Fig 7A) to the cumulative proportion of transcription induction for cells bearing the p*STL1* reporter; 90% of the transcribing cells initiate transcription at the start of the osmotic stress response, while Hog1 nuclear accumulation is rising and before it drops below 80% of its maximum (decay time). A similar behavior is observed for all the promoters tested whether they display basal activity or not (Figure 3B). For p*ALD3*, which is the slowest promoter tested, 87% of the Start Times are detected before the decay of Hog1 activity at 0.2M NaCl (7 min) while the full adaptation time of the HOG pathway takes 14 min.

In parallel to this observation, the productivity of the transcriptional output decreases with the time after the stimulus. Cells that start transcribing the p*STL1* promoter early, display a larger integral over the PP7 signal and a higher maximum intensity compared to cells that initiate transcription later (Figure 3C and Supplementary Fig 7B). A similar behavior is quantified for all tested promoters, independently of the presence or absence of basal transcription (Supplementary Fig 7C and D). These measurements demonstrate that the high Hog1 nuclear activity present in the first minutes of the response is key to determine the transcriptional state and the overall output of a promoter. If a locus has not been activated within these first minutes, it remains silent, despite the sustained presence of the active MAPK in the nucleus. In addition, the later the promoter activation takes place, the lower the output of the transcription will be, consistent with the active role played by Hog1 in multiple steps of the transcription process, notably its recruitment and association with the elongation complex[41].

Transcription factors control the dynamics and level of mRNA production

We showed that chromatin state affects the probability and the dynamics of induction of osmostress gene promoters. We have also observed that the time at which a locus is activated influences the level of transcription arising from this locus. In order to assess the transcriptional level of each promoter, we use as a proxy the maximum of the PP7 trace of each single cell where a transcription event could be detected (Figure 4A). This value represents the maximal loading of polymerase on the locus taking place during the period of transcription. Similar results are obtained when comparing the integral below the PP7 trace, which represents the total transcriptional output from a promoter (Supplementary Fig 8A). Each promoter has a different intrinsic capability of inducing a given level of transcription, which is independent of the fact that the promoter possesses a basal transcriptional level or a fast activation. Indeed, p*GRE2* displays the lowest level of induction among the tested promoters, despite the presence of basal transcription arising from this promoter and being the second-fastest promoter tested.

As expected, the ability to recruit RNA polymerases is dependent on HOG activity. Indeed, the three promoters with basal activity display a much higher transcriptional activity upon 0.2M NaCl stress than in normal growth conditions (Figure 4B and Supplementary Fig 8B). This can be easily rationalized by the fact that additional transcription factors come into play to transduce the stress response signal into a gene expression program (Figure 1A). Osmostress genes are governed by five transcription factors (Hot1, Sko1, Smp1, Msn1 and Msn2/4)[35,42,43] and generally display a combination of their binding sites on their promoter sequences (Supplementary Fig 9).

Based on studies of synthetic promoters it has been established that binding sites number and distance from the transcription start site (TSS) influence the promoter output[44]. Unfortunately, endogenous osmostress promoters display a wide diversity in number and affinity of TF binding sites. Therefore, no obvious prediction of the transcriptional activity for osmostress promoters can be drawn. For instance, eight sites can be mapped on p*ALD3* and nine on p*CTT1*; however, p*CTT1* displays a much weaker output than p*ALD3*.

To test the implication of transcription factors on the transcription dynamics, *HOT1* and *SKO1* genes were deleted in the p*STL1* and p*GPD1* reporter strains (Figure 4C). As expected, deletion of either TF leads to a slower activation and decreased transcriptional output for both promoters (Figure 4D and E). This is consistent with a synergistic effect of multiple TFs on a promoter for recruiting Hog1, which will in turn determine the RNA PolII recruitment. For both promoters, deletion of *HOT1* has a stronger effect than *SKO1* deletion. For p*STL1*, the fraction of responding cells drops below 5% in the *hot1Δ* background (Figure 4F). For p*GPD1*, the fraction of responding cells remains higher than 90% for either TF deletions. Interestingly, more cells with basal expression were observed in the *sko1Δ* cells compared to the WT. This observation is in agreement with data showing that Sko1 is part of a repressor complex under log-phase growth and turned into an activator by Hog1 activity[45]. In addition, these results attest the key role played by the TF in controlling both the dynamics and level of transcription from these stress promoters.

Multiple polymerase convoys transcribe stress-responsive genes

In order to identify transcriptional bursts, we sought to identify strong fluctuations in each single-cell trace. Individual peaks, identified with the *findpeak* algorithm in Matlab, were filtered to retain only peaks separated by pronounced troughs (Methods). In 20 to 30% of the traces, 2 or more peaks were identified (Figure 5A and B). The total length of the transcript downstream of the promoter is 8kb (1.5 for the stem loops + 6.5 for the *GLT1* ORF). Based on a transcription speed of 20bp/s[19], the expected lifetime of a transcript in the TS is 6.6 min. This corresponds well to the mean duration observed for the p*ALD3*, p*CTT1*, p*STL1* and p*GRE2* reporters (Figure 5C). However, it is very unlikely that the strong TS intensities recorded are generated by a single transcript, but rather by a group of PolII that simultaneously transcribes the locus, probably forming convoys of polymerases[46]. Indeed, single mRNA FISH experiments have shown that following a 0.2M NaCl stress, the endogenous *STL1* locus produces on average 20 mRNAs per cell, but some cells can produce up to 100[47].

For p*HSP12* and p*GPD1*, the average peak duration is longer than 11 min (Figure 5C), suggesting that multiple convoys of polymerases are traveling consecutively through the ORF. Unfortunately, the long half-life of the transcripts on the locus prevents a separation of individual groups of polymerases. However, when the traces where multiple peaks were identified are analyzed separately, the mean duration of the pulses becomes closer to the expected value of 6.6 min (Figure 5D). In addition, the output of the transcription estimated by the maximum intensity of the trace or the integral under the whole curve is equal or lower for traces with multiple pulses compared to traces where only a single peak is present (Figure 5E and Supplementary Fig 10). Together these data strengthen the notion that these stress-responsive promoters are highly

processive, displaying a high rate of transcription once activated. Multiple convoys of polymerases can be present on the transcribed locus. In some instances, the pause between two identified convoys is long enough for our assay to detect them and these cells tend to have a decreased transcriptional output. Conversely, traces where no pauses are detected tend to have a higher maximum loading of polymerases and higher mRNA production outputs, as quantified by the trace maximum intensity and the trace integral, which suggests a higher polymerase convoy loading frequency.

Transcription shutoff is controlled by MAPK activity and promoter identity

We have shown that transcription initiation is dictated by early Hog1 activity. Next, we wanted to assess what are the determinants of transcriptional termination and by extension, the duration of transcriptional activity. In the HOG pathway, the duration of transcription has been reported to be limited by the cellular adaptation time. Therefore, the duration of transcription is shorter after a 0.1M NaCl stress and longer after a 0.3M stress, compared to a 0.2M stress (Figure 6A). For the p*STL1* promoter, the last time point where we detect the PP7 signal at the TS (EndTime) matches the timing of nuclear exit of the MAPK Hog1 at all concentrations tested (Figure 6B).

In order to challenge this correlation between Hog1 activity and transcription arrest, we sought to modulate the MAPK activity pattern by controlling the cellular environment in a dynamic manner. Using a flow channel set-up, we generated a step, a pulse, or a ramp in NaCl concentration (Figure 6C, Methods). This experiment was performed in a strain carrying the p*STL1*-PP7sl reporter in conjunction with a Hog1-mCherry allowing to monitor the kinase activity and the downstream transcriptional response in the same cell. The step stimulus at 0.2M NaCl corresponds approximately to the experiments performed in wells where the concentration of the osmolyte is suddenly increased at time zero and then stays constant for the remaining of the experiments (Supplementary Movie 3). In the pulse assay, after 7 min at 0.2M, the NaCl concentration is set back to 0M (Supplementary Movie 4). Consequently, this shortens the MAPK activity of Hog1 which leaves the nucleus when cells are back in the normal growth medium. The ramp experiment starts with a pulse at 0.2M NaCl, then the concentration is slowly increased to 0.6M NaCl over the next 20 min (Supplementary Movie 5). This constant rise in external osmolarity extends the activity window of Hog1 by preventing the adaptation of the cells. The transcriptional response from the *STL1* promoter follows generally the Hog1 activity pattern. Consequently, the PP7 signal is shortened in the pulse experiment and prolonged in the ramping conditions, compared to the step experiment (Figure 6C, lower panel).

The measured CDF of Start Time for the three different experimental conditions are identical up to the fifth minute (Figure 6D). In the pulse experiment, fewer cells become transcriptionally active because the MAPK activity stops early on. Conversely, the period of transcription activation is slightly extended in the ramp. However, even in this condition, we fail to activate transcription of the p*STL1* in all the cells. This is probably due to the fact that Hog1 activity is not maintained at its maximum for a sufficient time but drops progressively after 10 minutes (Figure 6C, middle panel). The End Times of transcription are clearly different for the three flow regimes, reflecting the activity windows provided by the MAPK in the different contexts (Figure 6E).

However, if we correlate the measured Hog1 adaptation time and the PP7 End Time in the same cell, the synchrony is only valid for the pulse experiment (Figure 6F). In the pulse, Hog1 activity drops when cells have initiated transcription. Removing the kinase from the nucleus has a direct impact on the transcriptional process which is halted within a few minutes after the end of the pulse. This experiment highlights the requirement for the active MAPK to be present throughout the transcriptional process. In the step and even more evidently in the ramp experiment, a global disconnection between Hog1 adaptation time and transcription End Time is observed. In the ramp conditions, in many cells, Hog1 has not adapted by the end of the time lapse, while transcription has already stopped much earlier. This observation indicates that an additional factor controls the transcriptional period which is linked to the ability to stochastically reinitiate multiple pulses of transcription after the initial strong pulse of signaling activity. A parameter which is essentially controlled by the promoter architecture of the gene.

In order to validate this observation, we quantified the duration of the transcriptional period in the six different promoters and plotted the cumulative distribution of End Times following a 0.2M NaCl stress (Figure 6G and H). Interestingly, despite the fact that all the adaptation times are similar for the different experiments, all six promoters display very different kinetics of inactivation, highlighting the contribution of the promoter identity on this parameter. Generally, promoters transcribed at a lower level (p*CTT1* and p*GRE2*) terminate transcription earlier. This shorter transcription window may reflect an inferior recruitment of activators of transcription on the promoter and thus allow for an earlier inhibition of transcription due to chromatin closure.

In addition, promoters possessing basal activity display an extended period of transcription after Hog1 adaptation time. For p*GPD1* and p*GRE2*, this results in a biphasic decay, where the first part of the decay corresponds to the arrest of Hog1-induced transcription and the second phase can be associated to the basal transcription arising from these promoters. Basal transcription may even be increased after the stress due to an elevated basal signaling activity of Hog1 in high osmotic conditions[48].

For p*HSP12*, transcription persists beyond the adaptation time of the cells, with nearly 30% of the cells that display an active TS at the end of the time lapse. This suggests that basal expression from this promoter is strongly increased post-stimulus. p*HSP12* possesses many Msn2/4 binding sites. Although the relocation dynamics of Hog1 and Msn2 are very similar during the adaptation phase, Msn2 displays some stochastic secondary pulses[26] not correlated to Hog1 relocation events (Supplementary Fig 1E and F) that could explain the stronger basal expression arising from this promoter post-adaptation.

Taken together, these measurements demonstrate that the MAPK activity pattern provides a temporal window where transcription can take place. When the signaling cascade is shut off, transcription ceases soon afterwards. However the promoter identity and probably its propensity to recruit positive activators will determine for how long the promoter can sustain an open chromatin environment favorable for transcription, while Hog1 activity decreases as cells adapt to their environment.

Discussion

In this study, we constructed PP7 reporter strains to monitor the transcription dynamics of osmostress promoters. Thanks to an automated analysis of time-lapse imaging datasets, highly dynamic measurements of mRNA production were extracted in hundreds of single cells. Osmotic shock is a transient stress which triggers the High Osmolarity Glycerol pathway. Glycerol accumulation shapes the cellular adaptation time and thus Hog1 activity window. In response to this signal, a large burst of mRNA arises from the stress promoters. This is typical of transmitted bursts, where the upstream signaling cascade or a regulatory network defines the period of transcriptional activity[20]. During this time, multiple convoys of polymerases transcribe the ORF. In many cases, these convoys are too closely spaced in time for our reporter to detect, however, when consecutive bursts can be identified, the overall transcriptional output is lower suggesting that a longer pause in transcription initiation has happened. In order to improve the identification of individual bursts, a shorter transcript could be placed after the PP7sl; however, it would decrease the brightness of the TS and thus the sensitivity of our assay.

We have observed that Hog1 activity can only induce transcription during the first minutes following the osmotic stress, corresponding to the phases when Hog1 nuclear enrichment increases and plateaus. A promoter that has not been induced during this time will remain inactive. MAPKs in general, and Hog1 in particular, have been shown to be tightly coupled to multiple steps of the transcription process[41,49]. Hog1 binds to the TF at the promoter, recruits the remodeling factors and acts as an elongation factor by associating with PolII. During the first few minutes of the stress response, Hog1 is active at the promoter in order to evict nucleosomes; subsequently the kinase moves to the ORF region to sustain the open chromatin state and enable an efficient transcription[33]. The implication of the MAPK on the ORF probably limits its ability to activate new loci once the maximum nuclear enrichment has been reached. On the transcribed ORF, two opposing activities are taking place: on the one hand, Hog1 promotes the transcription by sustaining an open chromatin environment. On the other hand, PolII recruits negative regulators of transcription, such as Ino80 and Set1. Ino80 is implicated in the redeposition of the nucleosome after the transcription[50], while Set1 methylates the nucleosome to deposit a repressive mark on the H3K4 residue[39]. The balance between these positive and negative regulators on the ORF can explain the relationship we observe between the Start Time and the transcriptional output. Because Hog1 activity decreases during the adaptation phase, the later an ORF becomes activated, the weaker, the Hog1 activity available to sustain its transcription.

The promoter architecture plays a major role in determining the transcriptional output from a gene. For stress-responsive genes, these sequences have to reach a balance between two contradictory requirements: repression during growth and fast activation upon stress. Among the six tested promoters, we find that three have a basal expression level leading to a low level of gene expression during normal growth and thus allowing rapid activation in the whole population. The three other promoters are strongly repressed during log-phase growth, however, upon stress, their activation is slower and even absent in 35–50% of the population. For each promoter, a trade-off has to be found between the level of repression under log-phase growth and the speed and variability in the gene expression upon stress. Interestingly, this status can be

449 modified by environmental cues since we have shown that by using an alternate
450 carbon source, we can induce basal expression from the usually repressed *STL1*
451 promoter and thus induce faster transcriptional activation upon osmotic shock.

452 In higher eukaryotes, the stress response MAPKs p38 and JNK relocate to the nucleus
453 upon activation[51,52]. Immediate early genes, such as c-Fos or c-Jun, are induced within
454 minutes after activation of MAPK cascades[3,54]. Interestingly, these loci display basal
455 expression and require minimal chromatin modification for their induction[53,55]. In
456 contrast, delayed primary response genes and secondary response genes require
457 more profound chromatin remodeling to induce their activation[54,56]. These similarities
458 between HOG transcriptional induction, where we identified two classes of promoters
459 based on their basal level and dynamics of induction, suggest a high conservation in
460 the mechanisms used by MAPK in all eukaryotes to regulate the dynamics of gene
461 expression.

462

463

464 Acknowledgment

465 We thank the Pelet lab and Martin lab and for helpful discussions. Marta Schmitt,
466 Gaëlle Spack, Joan Jordan and Clémence Varidel for technical assistance. David
467 Shore and his lab for helpful discussions and reagents. Marie-Pierre Peli-Gulli and
468 Claudio de Virgilio for plasmids, Tineke Lenstra for suggesting the PP7ΔFG allele.
469 Agathe Pelet for manual curation of microscopy images. Eulalia de Nadal, Mariona
470 Nadal-Ribelles and Veneta Gerganova for critically reading the manuscript. Work in
471 the Pelet lab is supported by SystemsX.ch (IPhD 51PHP0_157354), the Swiss
472 National Science Foundation (SNSF, PP00P3_172900 and 31003A_182431) and the
473 University of Lausanne.

474

475 Author Contributions

476 VW and SP designed the experiments, analyzed the data and wrote the manuscript.
477 SP performed the raffinose and the flow experiments. VW conducted all the other
478 experiments.

479

480 Declaration of Interests

481 The authors declare no competing interests.

482

483

Material and Methods

Plasmids and yeast strains

All plasmids used in this study are listed in Supplementary Table 1. The PP7-GFP plasmid are based on the bright and photostable GFPenvy fluorescent protein[29]. The PP7 protein contains a truncation in the capsid assembly domain (PP7ΔFG residues 67–75: CSTSVCGE). Expression of the PP7 construct is controlled by a p*ADH1* promoter and a t*CYC1* terminator. The final construct pVW284 is cloned in a single integration vector URA3 (pSIVu[57] Addgene #81089). The PP7 stem loops plasmids are based on the previously published p*POL1* 24x*PP7sl* integrative plasmid[19] (Addgene 35196). The stress responsive promoters replace the pPOL1 promoter in the original construct using 1 kbp (800 bp for p*STL1*) upstream of the ATG codon. The PP7 reporter plasmids are available on Addgene.

All strains were constructed in the W303 background and are listed in Supplementary Table 2. Transformations were performed with standard lithium-acetate protocols. Gene deletions and gene tagging were performed with either pFA6a cassettes[58,59] or pGT cassettes[57]. Transformants were selected with auxotrophy markers (Uracil, Histidine, Leucine and Tryptophan) and gene deletions were performed with antibiotic resistance to Nourseothricin (NAT), to a concentration of 100 μg/ml. A fluorescently tagged histone strain was transformed with the PP7-GFP plasmid for integration in the *URA3* locus. Transformants were screened by microscopy for single integration. The selected strain was transformed with different osmostress promoters driving PP7sl plasmids linearized with a NotI digestion and integrated upstream of the *GLT1* ORF, as previously published[19]. Correct integration into the *GLT1* locus was screened by colony PCR with primers in the *GLT1* ORF (+600 bp) and in the *TEF* terminator of the selection marker on genomic DNA extraction. The integrity of the PP7 stem-loops array was assessed within the *TEF* terminator and in *GLT1* ORF (+250 bp) primers for all the promoters and deletions, after each transformation performed. For strains used in the study, at least two clones with correct genotypes were isolated and tested during a salt challenge time-lapse experiment. From the data analysis, the most frequent phenotype was isolated and the strain selected.

Yeast culture

Yeast cells were grown in YPD medium (YEP Broth: CCM0405, ForMedium) for transformation or in Synthetic Defined (SD) medium (YNB:CYN3801/CSM : DCS0521, ForMedium). For time-lapse experiments, cells were grown at least 24 hours in log-phase. A saturated overnight culture in SD medium was diluted into fresh SD-full medium to OD_{600} 0.025 in the morning and grown for roughly 8 hours to reach OD_{600} 0.3-0.5. In the evening cultures were diluted by adding $(0.5/OD_{600})\mu$l of cultures in 5ml SD-full for an overnight growth that kept cells in log-phase conditions. Cultures reached an OD_{600} of 0.1-0.3 in the morning of the second day and further diluted if necessary to remain below an OD_{600} of 0.4 during the day.

To prepare the samples for the microscopy experiments, these cells grown in log-phase for at least 24 hours were diluted to an OD_{600} 0.05 and sonicated twice 1 min before placing 200 μl of culture into the well of a 96-well glass bottom plate (MGB096-

1-2LG, Matrical Bioscience) previously coated with a filtered solution of Concanavalin A diluted to 0.5mg/ml in water (C2010, Sigma-Aldrich)[60]. Cells were let to settle for 30–45 minutes before imaging. Osmotic shock was performed under the microscope into the 96-well plate, by adding 100 μl of a three times concentrated SD-full+NaCl stock solutions to the 200 μl of medium already in the well, to reach the final desired salt concentration.

Microscopy

Images were acquired on a fully automated inverted epi-fluorescence microscope (Ti2-Eclipse, Nikon) placed by an incubation chamber set at 30 °C. Excitation was provided by a solid-state light source (SpectraX, Lumencor) and dedicated filter sets were used to excite and detect the proper fluorescence wavelengths with a sCMOS camera (Flash 4.0, Hamamatsu). A motorized XY-stage was used to acquire multiple filed of views in parallel and a piezo Z-stage (Nano-Z200, Mad City Labs) allowed fast Z-dimension scanning. Micro-manager was used to control the multidimensional acquisitions[61].

Experiments with PP7sl were acquired with a 60X oil objective. For strains with PP7-GFP and Hta2-mCherry, GFP (40ms, 3% LED power) and RFP (20ms), along with two bright field images were recorded every 15 seconds for the GFP and every minute for the other channels, for a total duration of 25 minutes. Six z-stacks were performed on the GFP channels covering ±1.2 μm from the central plane with 0.4 μm steps. An average bleaching of 32% for the GFP and 26% for the RFP for the whole time-lapse was quantified, in a strain without the PP7 stem loops, to avoid artifacts from the appearance of bright fluorescent foci. For all time-lapse experiments, media addition was performed before time point 4, defined as time zero.

Data analysis

Time-lapse movies were analyzed in an automated way: cell segmentation, tracking and feature measurements were performed by the YeastQuant platform[30]. All PP7 experiments were realized in at least two or three fully independent replicate experiments. A representative experiment was selected for each strain and inducing conditions, based on cell size and cell adaptation dynamics. The replicates which did not pass one of these controls were discarded from the replicate analyses. Individual single cell traces were filtered based on cell shape and GFP intensity to remove segmentation errors or other experimental artifacts. In addition, cells in mitosis were removed from the analysis with a 0.95 filter on the nuclei eccentricity, to remove artifacts from locus and PP7 signal duplication.

The Hta2 signal combined with the two bright field images allowed to define the nucleus and cell borders. The GFP z-stacks were converted by a maximum intensity projection in a single image that was used for quantification. In order to avoid improper quantification of transcription sites at the nuclear periphery, the Nucleus object defined by the histone fluorescence was expanded by 5 pixels within the Cell object to define the ExpNucl object. The transcription site intensity was quantified by the difference between the mean intensity of the 20 brightest pixels in the ExpNucl (HiPix) and the average intensity from the same region. This provides a continuous trace which is

close to zero in absence of TS and increases by up to few hundred counts when a TS is present. To identify the presence of a transcription site, a second feature named ConnectedHiPix was used (Supplementary Fig 4A). Starting from the 20 HiPix a morphological opening of the image was performed to remove isolated pixels and retaining only the ones that clustered together which correspond to the transcription site. The ConnectedHiPix value was set to the mean intensity of the pixel present in the largest object remaining after the morphological operation. If no pixel remained after the morphological operation, the ConnectedHiPix was set to NaN. In each single cell trace, ConnectedHiPix values only detected for a single time point were removed. After this filtering, the first and last time points where a ConnectedHiPix was measured were defined as transcription initiation (Start Time) and termination times (End Time) respectively. Manual curation of Start and End Times from raw microscopy images was performed to validate this transcription site detection strategy (Supplementary Fig 4B and C). In order to detect individual transcriptional bursts in the HiPix traces, the *findpeak* algorithm was used to identify all the peaks in the trace larger than a threshold of 7 counts within the Start and End Times. Following this first process, a set of conditions were defined to retain only the more reliable fluctuations: the drop following the peak has to be larger the fourth of the peak intensity; the intensity of the following peak has to rise by more than a third of the value at the trough. In addition, the value of the peak has to be at least one fifth of the maximum intensity of the trace in order to remove small intensity fluctuations being considered as peaks.

Raffinose experiment

For the experiments comparing p*STL1*-PP7sl induction in glucose versus raffinose, cells were grown overnight to saturation in SD-full medium. The cultures were diluted to OD 0.025 (Glucose) or 0.05 (Raffinose) and grown at 30° for at least four hours. In the raffinose medium, the expression level of the PP7-GFP was 2-fold lower than in glucose. Because of this low fluorescence intensity, cells were imaged with a 40X objective, and a single Z plane was acquired. Manual curation of the images was performed to define the Start Time in more than 250 cells. This experiment was performed in duplicate.

Flow chamber experiment

The flow experiments were performed in Ibidi chambers (*μ*-Slide VI 0.4, Ibidi). Two 50ml Falcon tube reservoirs containing SD-full + 0.5 *μ*g/ml fluorescein-dextran (D3305, ThermoFischer) and SD-full + 0.6 M NaCl were put under a pressure of 30mbar (FlowEZ, Fluigent). The media coming from each reservoir were connected using FEP tubing (1/16" OD x 0.020" ID, Fluigent) to a 3-way valve (2-switch, Fluigent). The concentration of NaCl in the medium was controlled using a Pulse-Width Modulation strategy[62,63]. Periods of 4 seconds were used and within this time, the valve controlled the fraction of time when SD-full versus SD-full + NaCl was flowing. TTL signals generated by an Arduino Uno board and dedicated scripts were used to control precisely the switching of the valve. The fluorescein present in the SD-full medium quantified outside the Cell object provided an estimate of the NaCl concentration in the medium. Some strong fluctuations in this signal were probably generated by dust particles in the imaging oil or FLSN-dextran aggregates in the flow chamber. Following 24hrs log-phase growth, cells bearing the p*STL1*-PP7sl reporter, Hog1-mCherry and Hta2-tdiRFP tags were diluted to OD 0.2, briefly sonicated and loaded in an ibidi

channel previously coated by Concanavalin A. Cells were left to settle in the channel for 10 minutes before SD-full flow was started.

Figure Legends

Figure 1. Quantifying transcription in the HOG pathway.

A. Schematics of the transcriptional response induced by the MAPK Hog1 upon osmotic stress. Under normal growth conditions, the genomic locus is repressed by histones set in place by the Ino80 complex and Asf1/Rtt109. In addition, H3K4 methylated histone mediated by Set1 contributes to the repression of the locus (upper panel). When Hog1 is active (lower panel), it accumulates in the nucleus with the transcription factors Msn2/4. Hog1 binds to transcription factors Hot1 and Sko1, allowing the remodeling of the chromatin by Rpd3 and the SAGA complex. The polymerase can be recruited to the locus and the RSC and SWR complexes will evict nucleosomes on the ORF. **B.** Construction of the transcriptional reporter. The promoter of interest (pPROM) is cloned in front of 24 stem loops. This construct is transformed into yeast and integrates in the *GLT1* locus replacing the endogenous promoter. Upon induction of the promoter, the mRNA stem loops are transcribed and recognized by the fluorescently tagged PP7 phage coat protein. **C.** Maximum intensity projections of Z-stacks of microscopy images from the p*STL1*-PP7sl reporter system in a 0.2M NaCl osmotic stress time-lapse experiment. The appearance of bright foci (arrow heads) in the nucleus of the cells denotes the active transcription arising from the promoter. Scale bar 5 μm. **D.** Dynamics of the p*STL1*-PP7sl transcription site intensity (20 brightest pixels in the average fluorescence of the nucleus) following hyperosmotic stress. The mean from 200 to 400 cells is represented by the solid line. The shaded areas represent the SEM. **E.** Analysis of one representative single cell trace. The raw trace is smoothed with a moving average and normalized by subtracting the intensity of the first time point after the stimulus. Multiple quantitative values can be extracted from this trace.

Figure 2. Correlation between basal activity and transcription induction time.

A. Dynamics of the transcription site intensity from six different promoters following a 0.2M NaCl stress. The mean of at least 140 cells is represented by the solid line. The shaded areas represent the SEM. **B.** Percentage of cells where a PP7 TS site was detected. The light shaded area represents the percentage of PP7 positive cells before the stimulus was added (basal transcription). **C.** The microscopy thumbnails display cells bearing the p*GPD1*-PP7sl reporter system where transcription sites (arrow heads) can be detected before and after the stress of 0.2M NaCl. Scale bar 5 μm. **D.** Cumulative distribution function (CDF) of the Start Time for each promoter only for the cells that induce transcription after time zero. **E.** 10^{th}, 50^{th} and 90^{th} percentiles of the Start Times shown for the two to three replicates measured for each promoter. The number of stars next to each measurement corresponds to the number of promoters without basal level that are significantly different from the promoter with basal level (two-sample t-test, $p<0.05$). **F.** Cumulative distribution function of Start Times for the p*STL1*-PP7sl strain of wildtype, *htz1Δ* of *gcn5Δ* background. The inset shows the percentage of PP7 positive cells in each background. **G.** Cumulative distribution function of Start Times for the p*STL1*-PP7sl strain grown in glucose or raffinose. The

inset shows the percentage of PP7 positive cells, the light blue bar the basal positive PP7 cells.

Figure 3. Relationship between Start Time and Hog1 relocation dynamics.

A. In single cell Hog1 nuclear relocation traces, the timing of Hog1 nuclear entry (■), maximum enrichment (●), start of the decay in nuclear enrichment (◆) and Hog1 adaptation (▲) can be identified (upper panel). The median (marker) and 25th to 75th percentiles (lines) for these measurements are plotted for three different osmotic stresses (central panel). The cumulative distribution function of Start Times for the p*STL1*-PP7sl reporter for these same three concentrations is plotted (lower panel). **B.** Histogram of Start Times following a 0.2M stress for the five other promoters tested. The vertical dashed line represents the median decay time of Hog1 measured at 0.2M. The number in the legend indicates the percentage of cells which have initiated transcription before the median Hog1 decay time. **C.** The population of p*STL1*-PP7sl positive cells is split in four quartiles based on their Start Time. The median (●) and 25th to 75th percentiles (line) of the integral of the PP7 trace is plotted for each quartile.

Figure 4. Intensity of transcription in transcription factor deletions

A. Violin plot of the trace intensity (maximum of the TS during the transcription period) for the six promoters after stimulation by 0.2M NaCl. Each dot represents the value calculated from a single cell. The solid line is the median and the dashed line the mean of the population. **B.** Comparison between the trace intensity in stimulated (0.2M NaCl) and unstimulated conditions (0.0M) for the three promoters displaying basal expression. **C.** — **F.** Effect of the deletions of the HOT1 and SKO1 transcription factor genes on the dynamics of transcription (C), cumulative distribution of Start Times (D), the trace intensity (E) and the percentage of responding cells for the p*STL1*-PP7sl and p*GPD1*-PP7sl reporter strains following a 0.2M NaCl stress for at least 200 cells. For the p*STL1*-PP7sl *hot1Δ* sample, 349 cells were analyzed with only 9 displaying a PP7 positive signal. This low number does not allow to draw a meaningful CDF curve in panel D.

Figure 5. Analysis of transcription bursts.

A. Percentage of cells where 1, 2 or 3 and more peaks are identified among the population of responding cells for the different promoters following a 0.2M NaCl stress. **B.** Examples of single cell traces displaying 1 or 2 peaks for the p*STL1*-PP7sl and the p*GPD1*-PP7sl reporter strains. **C.** Violin plot representing the Peak Duration. Each dot represents the value calculated for a single peak. The solid line is the median and the dashed line the mean of all the peaks measured. **D.** - **E.** The population of cells was split between cells displaying one peak and two or more peaks. The Peak Duration (D) and Trace Intensity (E) are plotted for the p*HSP12*-PP7sl and p*GPD1*-PP7sl strains. Each dot represents the value calculated for a single peak (D) or a single cell (E). The solid line is the median and the dashed line the mean of the population.

Figure 6. Hog1 activity and promoter identity control the shutoff of transcription

A. Violin plot representing the Transcription Period (time difference between End Time and Start Time) measured for the p*STL1*-PP7sl reporter following 0.1, 0.2 and 0.3M NaCl stresses. Each dot represents the value calculated from a single cell. The solid line is the median and the dashed line the mean of the population. **B.** One minus the cumulative distribution function of End Times for the p*STL1*-PP7sl reporter. The

vertical dashed lines represent the median adaptation time of Hog1 for the three different stress levels. **C.** Dynamics of the estimated NaCl concentration in the medium for the pulse, step and ramp experiment protocols (upper panel, Methods). Corresponding Hog1 relocation dynamics (middle panel) and p*STL1*-PP7sl transcription site intensity (lower panel). The mean of at least 180 cells is represented by the solid line. The shaded areas represent the SEM. **D.** Cumulative distribution function (CDF) of the Start Time for all cells in the pulse, step and ramp experiments. The CDF at 15 min represents the fraction of responding cells for each condition. **E.** One minus the cumulative distribution function of End Times only for the responding cells in the pulse, step and ramp experiments. **F.** Correlation between the Hog1 adaptation time and the PP7 End Time measured in the same cells in the pulse, step and ramp experiments. The open markers indicate cells where Hog1 has not adapted at the end of the time lapse. Adaptation time is arbitrarily set to 35 min for this sub-population. **G.** Violin plot representing the Transcription Period measured for the six different promoters following a 0.2 NaCl stress. Each dot represents the value calculated from a single cell. The solid line is the median and the dashed line the mean of the population. **H.** One minus the cumulative distribution function of End Times for the different promoters. The vertical dashed line represents the median adaptation time of Hog1 at 0.2M NaCl.

Reference

1. Gasch, A. P. *et al.* Genomic expression programs in the response of yeast cells to environmental changes. *Mol Biol Cell* **11**, 4241–4257 (2000).
2. Roberts, C. J. *et al.* Signaling and circuitry of multiple MAPK pathways revealed by a matrix of global gene expression profiles. *Science* **287**, 873–880 (2000).
3. Ferreiro, I. *et al.* Whole genome analysis of p38 SAPK-mediated gene expression upon stress. *BMC Genomics* **11**, 144 (2010).
4. Berry, D. B. & Gasch, A. P. Stress-activated genomic expression changes serve a preparative role for impending stress in yeast. *Mol Biol Cell* **19**, 4580–4587 (2008).
5. Chen, R. E., Patterson, J. C., Goupil, L. S. & Thorner, J. Dynamic localization of Fus3 mitogen-activated protein kinase is necessary to evoke appropriate responses and avoid cytotoxic effects. *Mol Cell Biol* **30**, 4293–4307 (2010).
6. Formstecher, E. *et al.* PEA-15 Mediates Cytoplasmic Sequestration of ERK MAP Kinase. *Developmental Cell* **1**, 239–250 (2001).
7. Raser, J. M. & O'Shea, Erin K. Control of stochasticity in eukaryotic gene expression. *Science* **304**, 1811–1814 (2004).
8. Colman-Lerner, A. *et al.* Regulated cell-to-cell variation in a cell-fate decision system. *Nature* **437**, 699–706 (2005).
9. Pelet, S. *et al.* Transient activation of the HOG MAPK pathway regulates bimodal gene expression. *Science* **332**, 732–735 (2011).
10. Corrigan, A. M. & Chubb, J. R. Regulation of Transcriptional Bursting by a Naturally Oscillating Signal. *Current Biology* **24**, 205–211 (2014).
11. Roux, P. P. & Blenis, J. ERK and p38 MAPK-Activated Protein Kinases: a Family of Protein Kinases with Diverse Biological Functions. *Microbiology and Molecular Biology Reviews* **68**, 320–344 (2004).
12. Chen, R. E. & Thorner, J. Function and regulation in MAPK signaling pathways: lessons learned from the yeast Saccharomyces cerevisiae. *Biochim Biophys Acta* **1773**, 1311–1340 (2007).
13. Saito, H. & Posas, F. Response to hyperosmotic stress. *Genetics* **192**, 289–318 (2012).
14. Hohmann, S., Krantz, M. & Nordlander, B. Yeast osmoregulation. *Meth Enzymol* **428**, 29–45 (2007).
15. de Nadal, E. & Posas, F. Multilayered control of gene expression by stress-activated protein kinases. *EMBO J* **29**, 4–13 (2010).

16. de Nadal, E., Ammerer, G. & Posas, F. Controlling gene expression in response to stress. *Nat Rev Genet* **12**, 833–845 (2011).
17. Neuert, G. *et al.* Systematic Identification of Signal-Activated Stochastic Gene Regulation. *Science* **339**, 584–587 (2013).
18. Bertrand, E. *et al.* Localization of ASH1 mRNA particles in living yeast. *Mol Cell* **2**, 437–445 (1998).
19. Larson, D. R., Zenklusen, D., Wu, B., Chao, J. A. & Singer, R. H. Real-Time Observation of Transcription Initiation and Elongation on an Endogenous Yeast Gene. *Science* **332**, 475–478 (2011).
20. Lionnet, T. & Singer, R. H. Transcription goes digital. *EMBO Rep* **13**, 313–321 (2012).
21. Fritzsch, C. *et al.* Estrogen-dependent control and cell-to-cell variability of transcriptional bursting. *Molecular Systems Biology* **14**, e7678 (2018).
22. Zoller, B., Little, S. C. & Gregor, T. Diverse Spatial Expression Patterns Emerge from Unified Kinetics of Transcriptional Bursting. *Cell* **175**, 835-847.e25 (2018).
23. Reiser, V., Ruis, H. & Ammerer, G. Kinase activity-dependent nuclear export opposes stress-induced nuclear accumulation and retention of Hog1 mitogen-activated protein kinase in the budding yeast Saccharomyces cerevisiae. *Mol Biol Cell* **10**, 1147–1161 (1999).
24. Muzzey, D., Gómez-Uribe, C. A., Mettetal, J. T. & van Oudenaarden, A. A systems-level analysis of perfect adaptation in yeast osmoregulation. *Cell* **138**, 160–171 (2009).
25. Görner, W. *et al.* Nuclear localization of the C2H2 zinc finger protein Msn2p is regulated by stress and protein kinase A activity. *Genes Dev.* **12**, 586–597 (1998).
26. Hao, N. & O'Shea, E. K. Signal-dependent dynamics of transcription factor translocation controls gene expression. *Nature Structural & Molecular Biology* **19**, 31–39 (2012).
27. O'Rourke, S. M. & Herskowitz, I. Unique and Redundant Roles for HOG MAPK Pathway Components as Revealed by Whole-Genome Expression Analysis. *MBoC* **15**, 532–542 (2003).
28. Chao, J. A., Patskovsky, Y., Almo, S. C. & Singer, R. H. Structural basis for the coevolution of a viral RNA–protein complex. *Nature Publishing Group* **15**, 103–105 (2007).
29. Slubowski, C. J., Funk, A. D., Roesner, J. M., Paulissen, S. M. & Huang, L. S. Plasmids for C-terminal tagging in Saccharomyces cerevisiaethat contain improved GFP proteins, Envy and Ivy. *Yeast* **32**, 379–387 (2015).
30. Pelet, S., Dechant, R., Lee, S. S., van Drogen, F. & Peter, M. An integrated image analysis platform to quantify signal transduction in single cells. *Integrative biology : quantitative biosciences from nano to macro* **4**, 1274–1282 (2012).
31. Munsky, B., Neuert, G. & van Oudenaarden, A. Using Gene Expression Noise to Understand Gene Regulation. *Science* **336**, 183–187 (2012).
32. de Nadal, E. *et al.* The MAPK Hog1 recruits Rpd3 histone deacetylase to activate osmoresponsive genes. *Nature* **427**, 370–374 (2004).
33. Mas, G. *et al.* Recruitment of a chromatin remodelling complex by the Hog1 MAP kinase to stress genes. *EMBO J* **28**, 326–336 (2009).
34. Aymoz, D., Wosika, V., Durandau, E. & Pelet, S. Real-time quantification of protein expression at the single-cell level via dynamic protein synthesis translocation reporters. *Nature Communications* **7**, 11304 (2016).
35. Rep, M. *et al.* Osmotic stress-induced gene expression in Saccharomyces cerevisiae requires Msn1p and the novel nuclear factor Hot1p. *Mol Cell Biol* **19**, 5474–5485 (1999).
36. Alepuz, P. M., de Nadal, E., Zapater, M., Ammerer, G. & Posas, F. Osmostress-induced transcription by Hot1 depends on a Hog1-mediated recruitment of the RNA Pol II. *EMBO J* **22**, 2433–2442 (2003).
37. Zapater, M., Sohrmann, M., Peter, M., Posas, F. & de Nadal, E. Selective requirement for SAGA in Hog1-mediated gene expression depending on the severity of the external osmostress conditions. *Mol Cell Biol* **27**, 3900–3910 (2007).
38. Wan, Y. *et al.* Role of the histone variant H2A.Z/Htz1p in TBP recruitment, chromatin dynamics, and regulated expression of oleate-responsive genes. *Mol Cell Biol* **29**, 2346–2358 (2009).
39. Nadal-Ribelles, M. *et al.* H3K4 monomethylation dictates nucleosome dynamics and chromatin remodeling at stress-responsive genes. *Nucleic Acids Research* **43**, 4937–4949 (2015).
40. Ferreira, C. & Lucas, C. Glucose repression over Saccharomyces cerevisiae glycerol/H+ symporter gene STL1 is overcome by high temperature. *FEBS Lett* **581**, 1923–1927 (2007).
41. Proft, M. *et al.* The stress-activated Hog1 kinase is a selective transcriptional elongation factor for genes responding to osmotic stress. *Mol Cell* **23**, 241–250 (2006).

42. de Nadal, E. & Posas, F. Regulation of gene expression in response to osmostress by the yeast stress-activated protein kinase Hog1. *Topics in Current Genetics* **20**, 81 (2008).
43. Capaldi, A. P. *et al.* Structure and function of a transcriptional network activated by the MAPK Hog1. *Nat Genet* **40**, 1300–1306 (2008).
44. Sharon, E. *et al.* Inferring gene regulatory logic from high-throughput measurements of thousands of systematically designed promoters. *Nat Biotechnol* **30**, 521–530 (2012).
45. Proft, M. & Struhl, K. Hog1 kinase converts the Sko1-Cyc8-Tup1 repressor complex into an activator that recruits SAGA and SWI/SNF in response to osmotic stress. *Mol Cell* **9**, 1307–1317 (2002).
46. Tantale, K. *et al.* A single-molecule view of transcription reveals convoys of RNA polymerases and multi-scale bursting. *Nature Communications* **7**, 12248 (2016).
47. Li, G. & Neuert, G. Multiplex RNA single molecule FISH of inducible mRNAs in single yeast cells. *Sci Data* **6**, 94 (2019).
48. Macia, J. *et al.* Dynamic signaling in the Hog1 MAPK pathway relies on high basal signal transduction. *Science Signaling* **2**, ra13 (2009).
49. Pokholok, D. K., Zeitlinger, J., Hannett, N. M., Reynolds, D. B. & Young, R. A. Activated signal transduction kinases frequently occupy target genes. *Science* **313**, 533–536 (2006).
50. Klopf, E. *et al.* Cooperation between the INO80 complex and histone chaperones determines adaptation of stress gene transcription in the yeast Saccharomyces cerevisiae. *Mol Cell Biol* **29**, 4994–5007 (2009).
51. Cavigelli, M., Dolfi, F., Claret, F. X. & Karin, M. Induction of c-fos expression through JNK-mediated TCF/Elk-1 phosphorylation. *The EMBO Journal* **14**, 5957–5964 (1995).
52. Wood, C. D., Thornton, T. M., Sabio, G., Davis, R. A. & Rincon, M. Nuclear Localization of p38 MAPK in Response to DNA Damage. *Int. J. Biol. Sci.* 428–437 (2009). doi:10.7150/ijbs.5.428
53. Fowler, T., Sen, R. & Roy, A. L. Regulation of Primary Response Genes. *Molecular Cell* **44**, 348–360 (2011).
54. Tullai, J. W. *et al.* Immediate-Early and Delayed Primary Response Genes Are Distinct in Function and Genomic Architecture. *J. Biol. Chem.* **282**, 23981–23995 (2007).
55. O'Donnell, A., Odrowaz, Z. A. & Sharrocks, A. D. Immediate-early gene activation by the MAPK pathways: what do and don't we know? *Biochemical Society transactions* **40**, 58–66 (2012).
56. Ramirez-Carrozzi, V. R. *et al.* Selective and antagonistic functions of SWI/SNF and Mi-2β nucleosome remodeling complexes during an inflammatory response. *Genes Dev.* **20**, 282–296 (2006).
57. Wosika, V. *et al.* New families of single integration vectors and gene tagging plasmids for genetic manipulations in budding yeast. *Molecular Genetics and Genomics* **291**, 2231–2240 (2016).
58. Goldstein, A. L. & McCusker, J. H. Three new dominant drug resistance cassettes for gene disruption in Saccharomyces cerevisiae. *Yeast* **15**, 1541–1553 (1999).
59. Sheff, M. A. & Thorn, K. S. Optimized cassettes for fluorescent protein tagging in Saccharomyces cerevisiae. *Yeast* **21**, 661–670 (2004).
60. Pelet, S., Aymoz, D. & Durandau, E. Temporal quantification of MAPK induced expression in single yeast cells. *J Vis Exp* (2013). doi:10.3791/50637
61. Edelstein, A., Amodaj, N., Hoover, K., Vale, R. & Stuurman, N. Computer control of microscopes using μManager. *Curr Protoc Mol Biol* **Chapter 14**, Unit14.20 (2010).
62. Unger, M., Lee, S.-S., Peter, M. & Koeppl, H. Pulse Width Modulation of Liquid Flows: Towards Dynamic Control of Cell Microenvironments. in *15th International Conference on miniaturized systems for chemistry and life sciences : Microtas 2011* 1567–1569 (Chemical and Biological Microsystems Society, 2011).
63. Unger, M. P. Interrogating the single cell: computational and experimental methods for optimal live cell experiments. (ETH Zurich, 2014). doi:10.3929/ethz-a-010350761

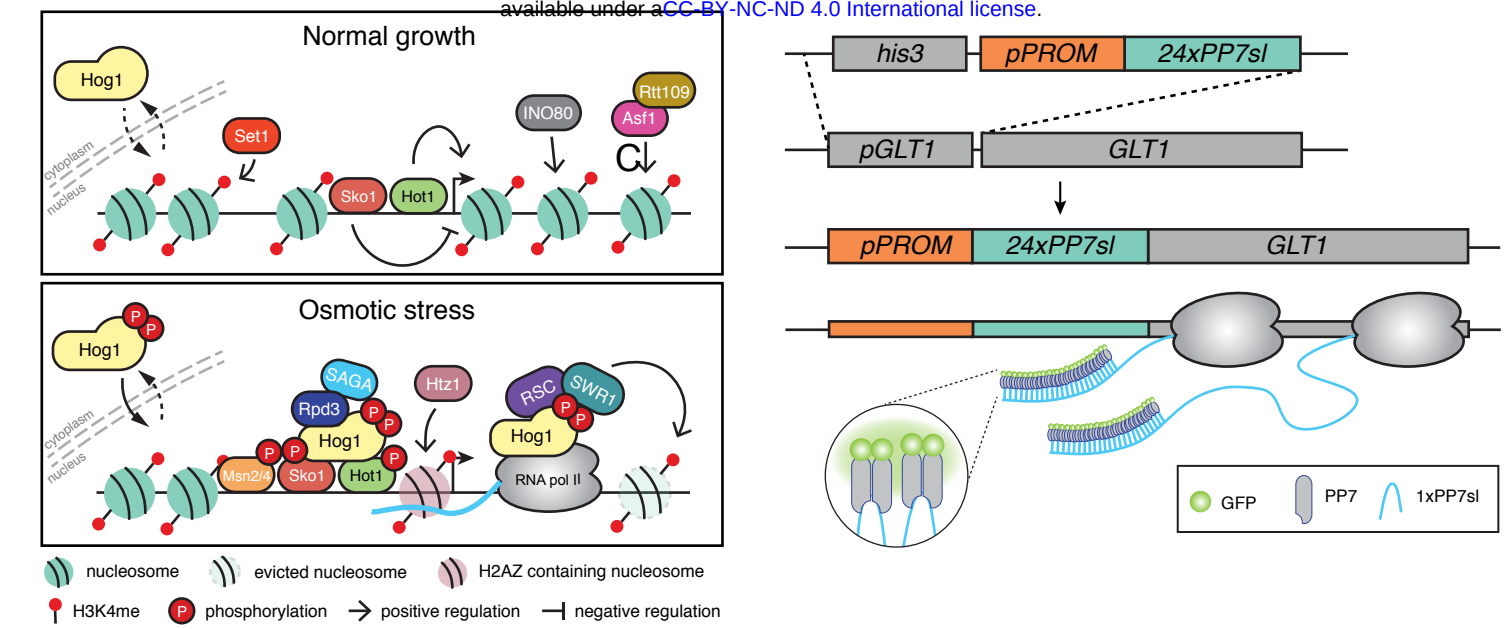

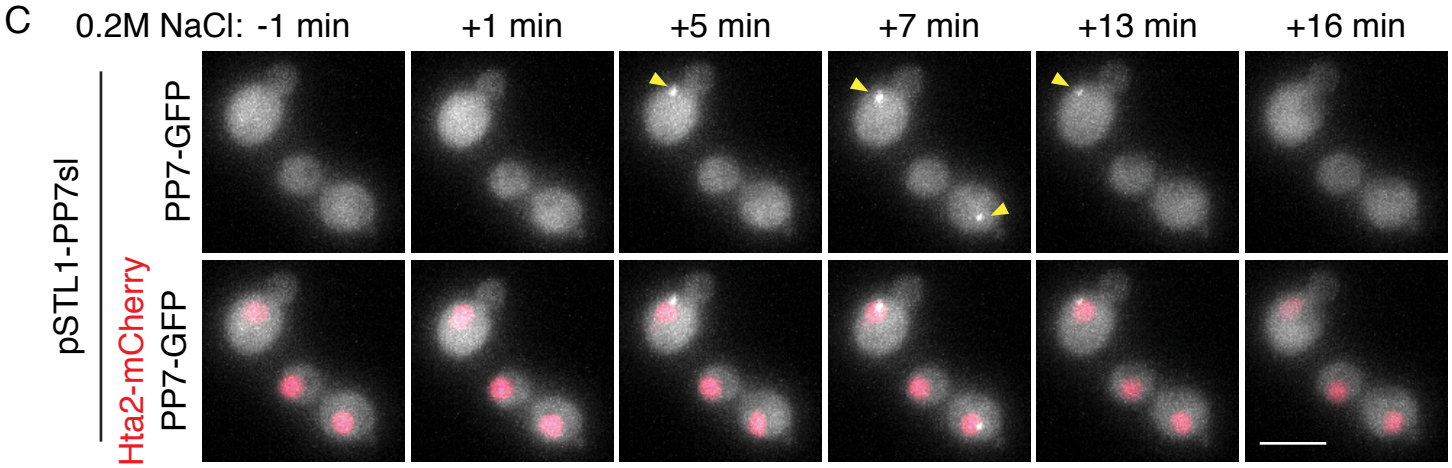

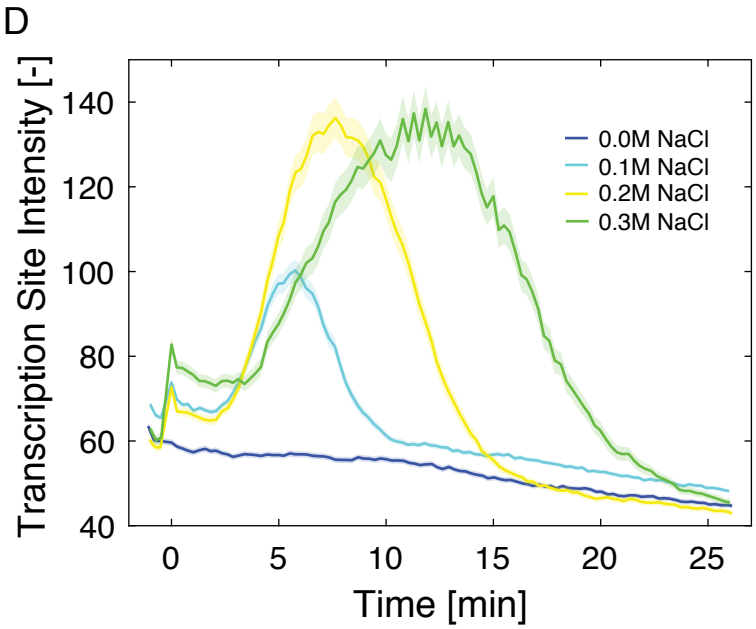

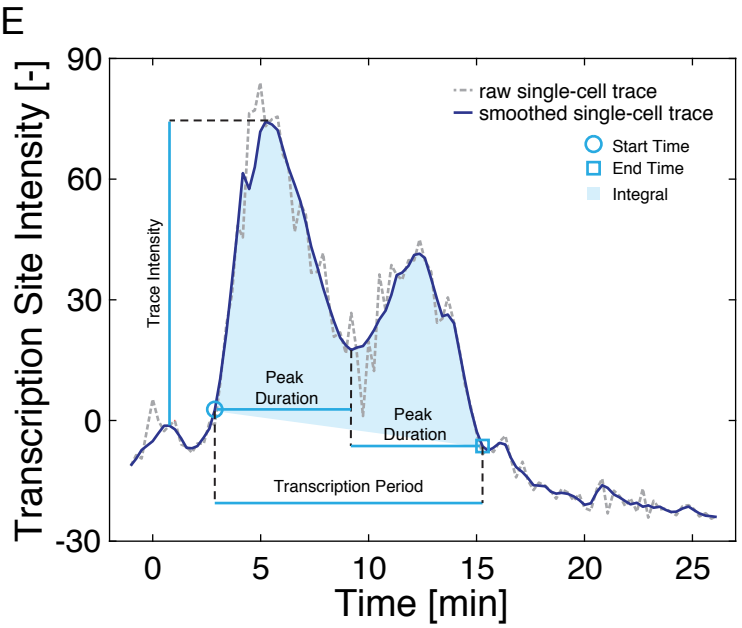

Figure 1

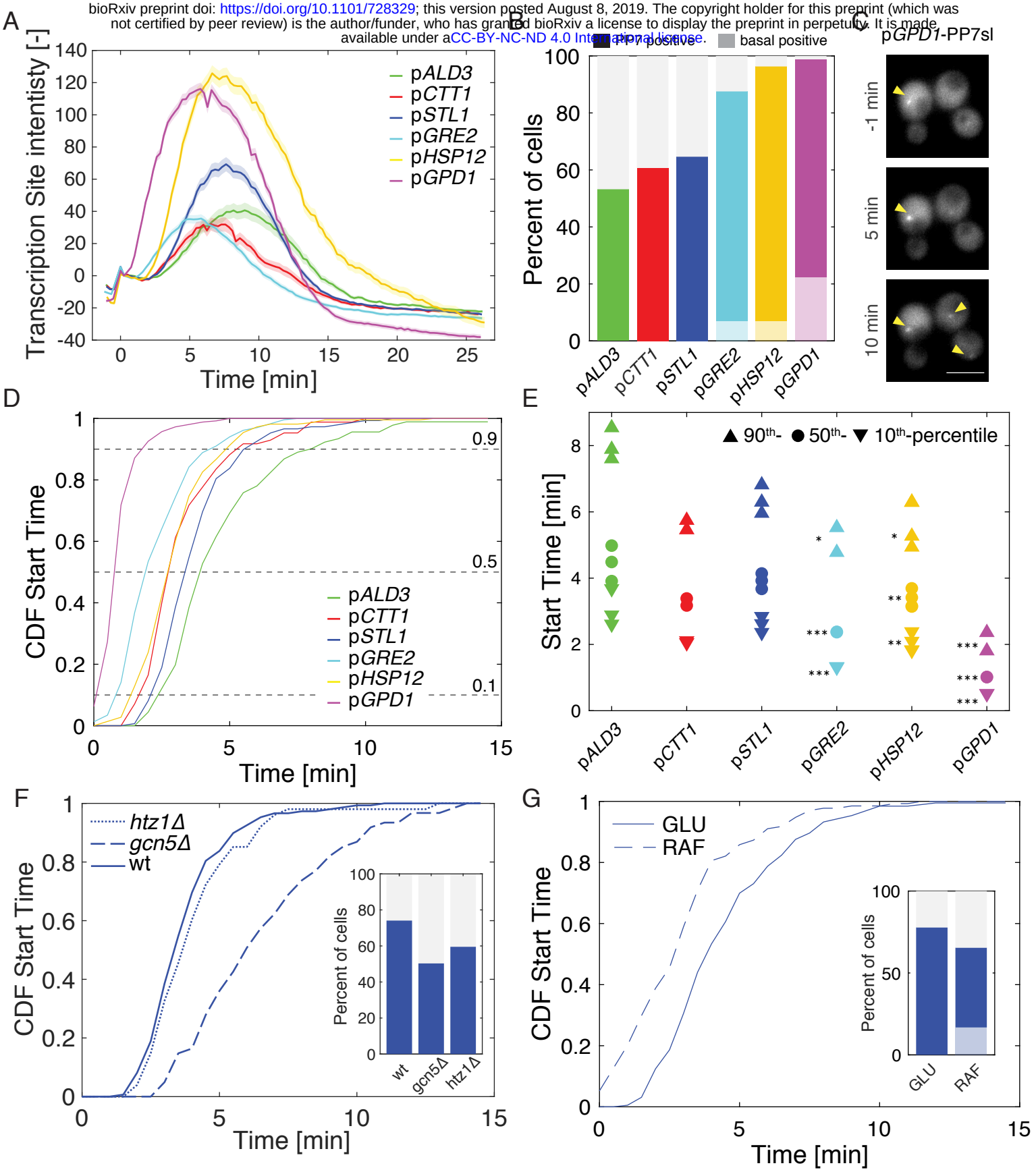

Figure 2

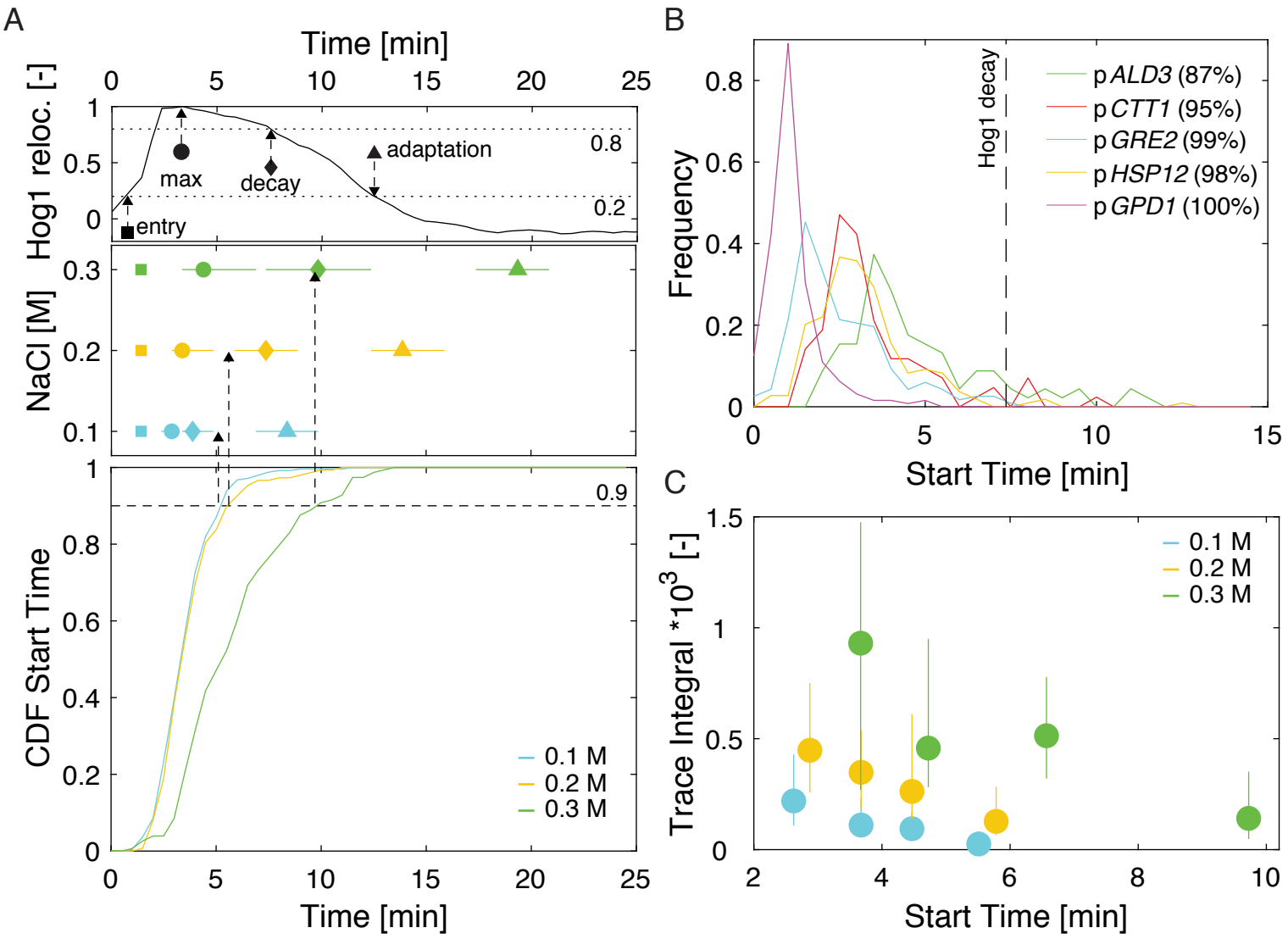

Figure 3

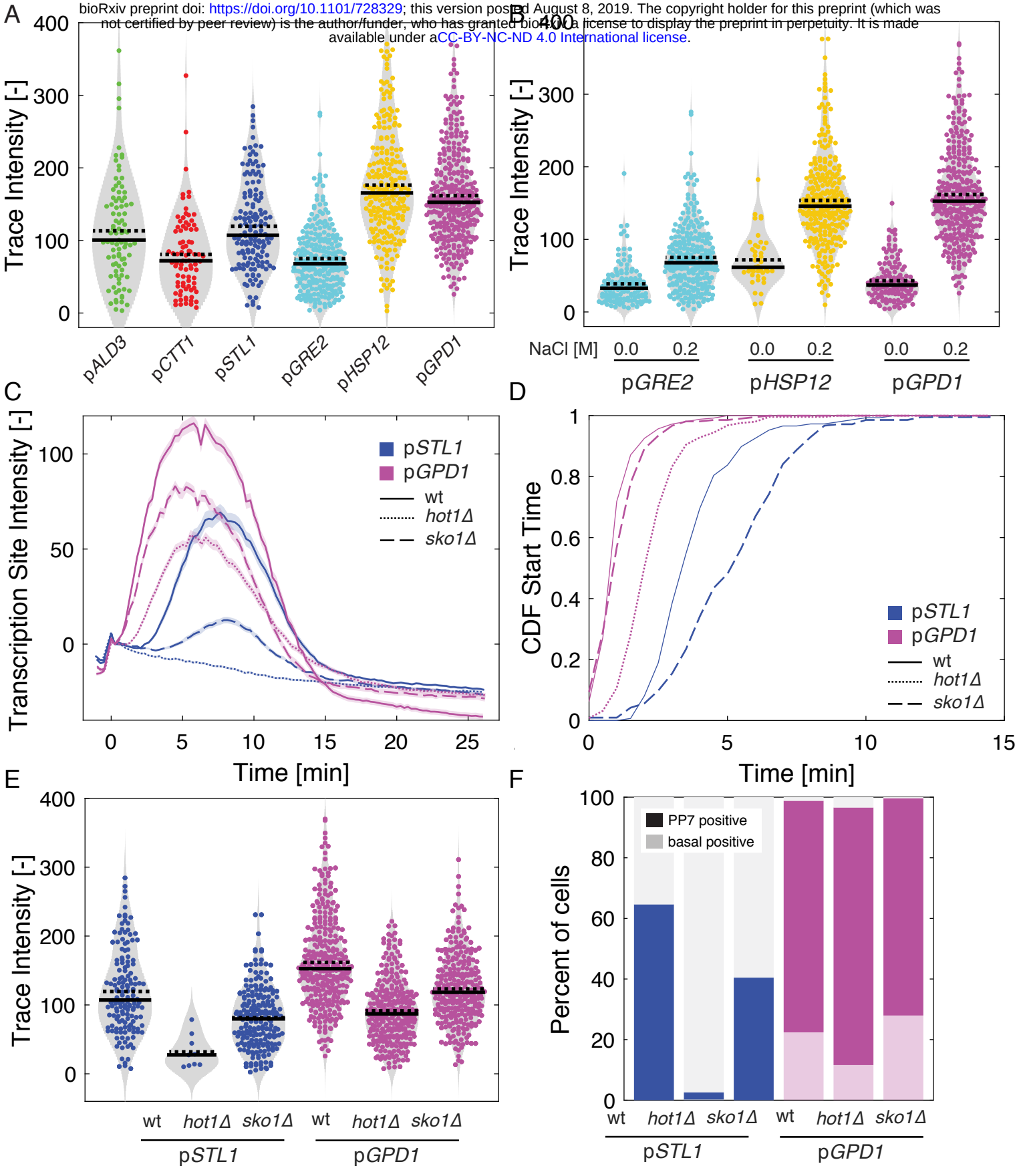

Figure 4

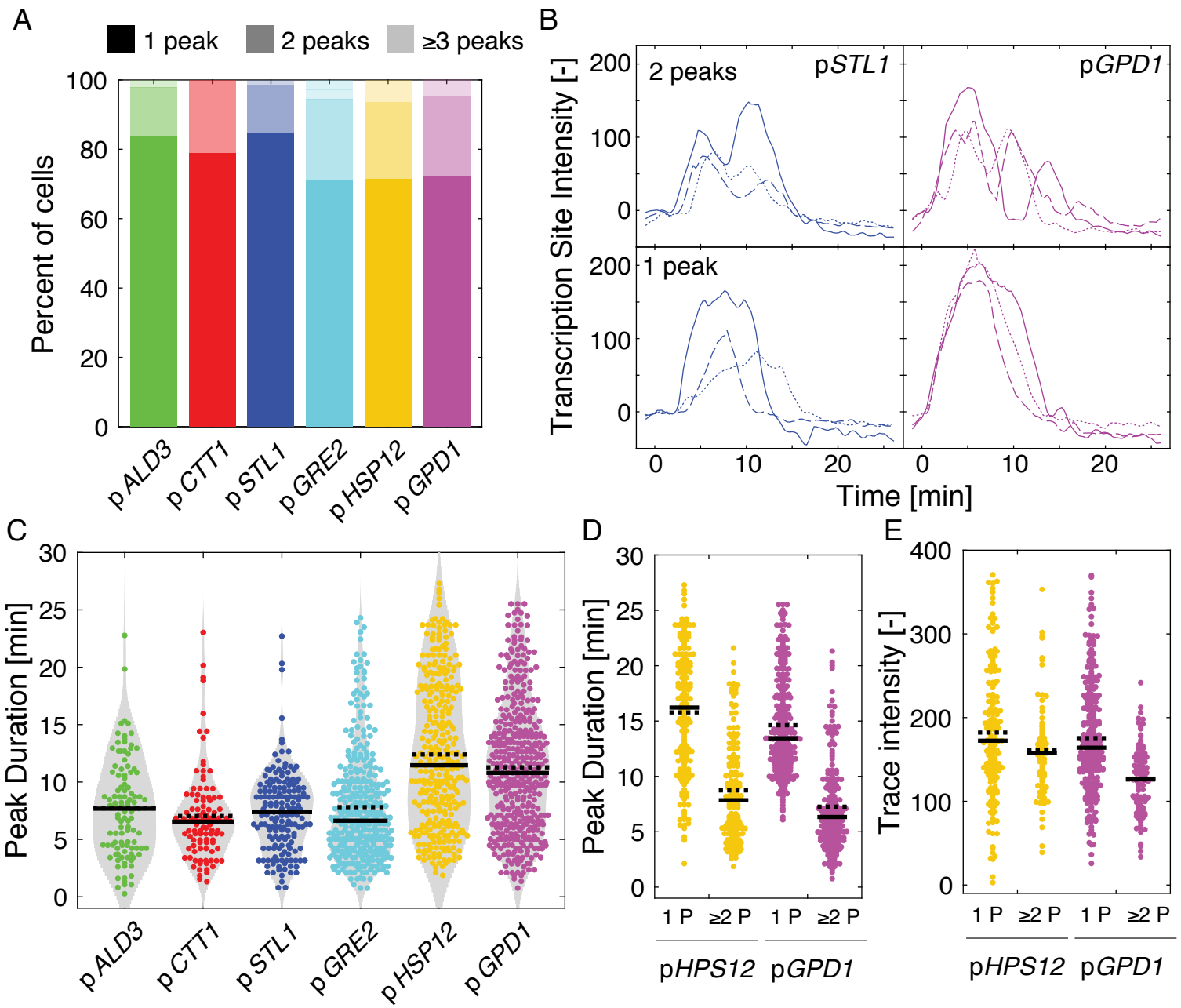

Figure 5

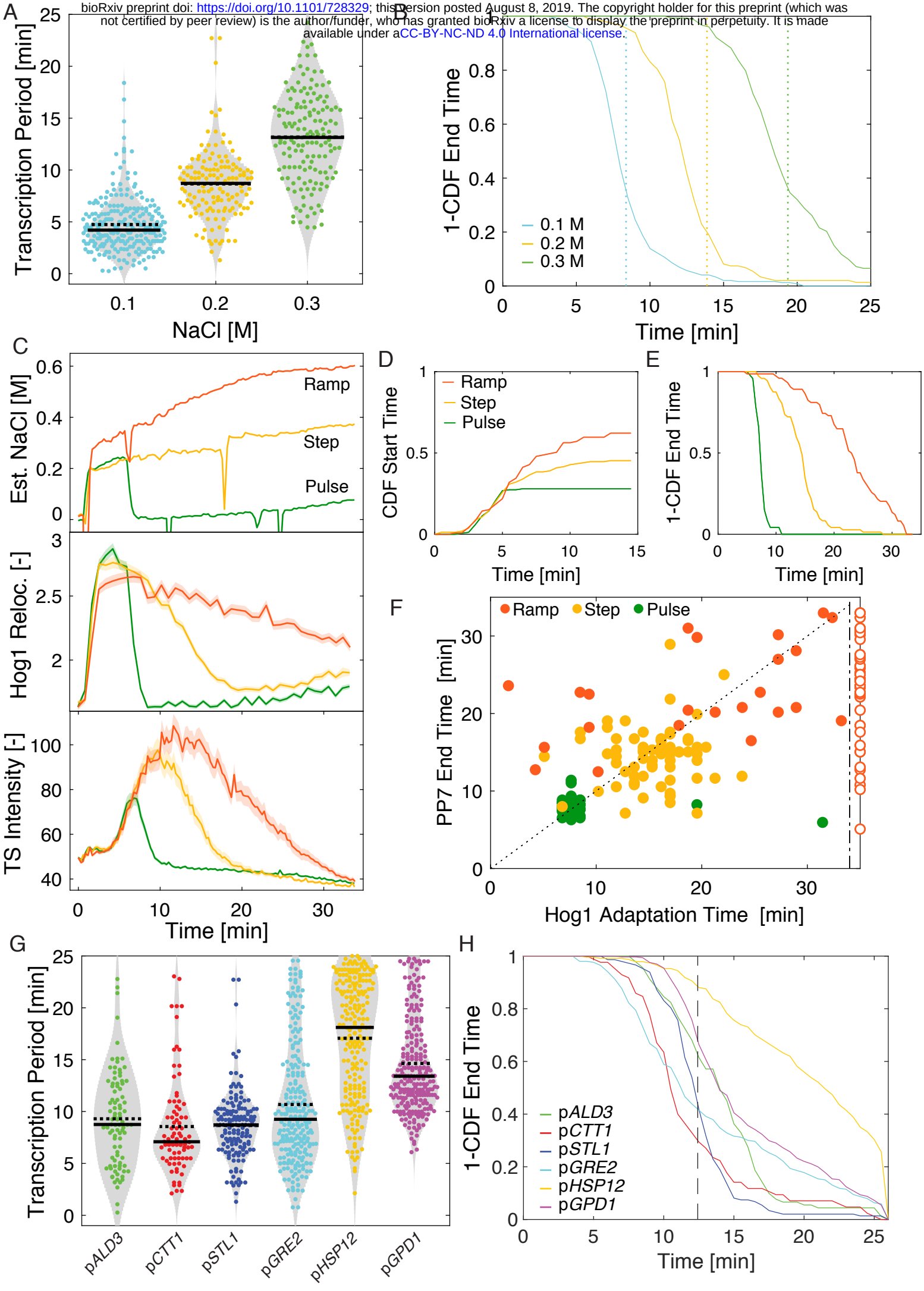

Figure 6